MHD stagnation point flow of viscoelastic nanofluid with non-linear radiation effects

Citation for published version:
Farooq, M, Khan, MI, Waqas, M, Hayat, T, Alsaedi, A & Khan, MI 2016, 'MHD stagnation point flow of viscoelastic nanofluid with non-linear radiation effects', *Journal of Molecular Liquids*, vol. 221, pp. 1097–1103. https://doi.org/10.1016/j.molliq.2016.06.077

Digital Object Identifier (DOI):
10.1016/j.molliq.2016.06.077

Link:
Link to publication record in Heriot-Watt Research Portal

Document Version:
Peer reviewed version

Published In:
Journal of Molecular Liquids

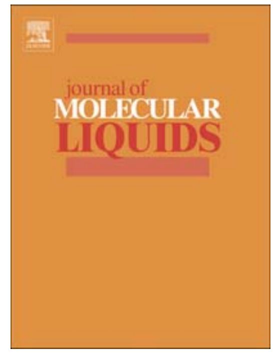

MHD stagnation point flow of viscoelastic nanofluid with non-linear radiation effects

M. Farooq, M. Ijaz Khan, M. Waqas, T. Hayat, A. Alsaedi, M. Imran Khan

PII: S0167-7322(16)31219-3
DOI: doi: 10.1016/j.molliq.2016.06.077
Reference: MOLLIQ 5984

To appear in: *Journal of Molecular Liquids*

Received date: 16 May 2016
Revised date: 29 May 2016
Accepted date: 22 June 2016

MHD stagnation point flow of viscoelastic nanofluid with non-linear radiation effects

M. Farooq[a], M. Ijaz Khan[b,1], M. Waqas[b], T. Hayat[b,c], A. Alsaedi[c] and M. Imran Khan[d]
[a]Department of Mathematics, Riphah International University, Islamabad 44000 Pakistan
[b]Department of Mathematics, Quaid-I-Azam University 45320, Islamabad 44000, Pakistan
[c]Nonlinear Analysis and Applied Mathematics (NAAM) Research Group, *Department of Mathematics, Faculty of Science, King Abdulaziz University, P. O. Box* 80203, *Jeddah* 21589, *Saudi Arabia*
Heriot Watt University, Edinburgh Campus, Edinburgh EH14 4AS, United Kingdom

Abstract: This article addresses MHD stagnation point flow of viscoelastic nanofluid towards a stretching surface with nonlinear radiative effects. Nanofluid model consists of Brownian motion and thermophoresis. Heat transfer is studied by employing convective condition at the stretching surface. Newly constructed condition for heat transfer is imposed. The relevant problems are modeled by considering nonlinear thermal radiation. Similarity transformation is utilized to reduce the nonlinear partial differential equations into coupled nonlinear ordinary differential equations. The convergent solutions for velocity, temperature and concentration equations developed. Graphical results are drawn for the velocity, temperature, concentration, skin friction coefficient and Nusselt number. It is noticed that skin friction increases for larger magnetic parameter.

Keywords: Non-linear radiative effect; viscoelastic fluid; Convective boundary condition

1.Introduction

The utilization of nanotechnology has attracted the attention of recent investigators since nanoscale materials owns chemical, electrical and unique optical properties. Recent advancements made it conceivable to diffuse nanoparticles in ordinary heat transfer liquids including engine oil, ethylene glycol and water to create another class of heat transfer liquids with great effectiveness. Liquids shaped of immersed fluid and suspended nanoparticles are called nanofluids. These liquids have much higher thermal conductivity when compared with traditional heat transfer liquids even at low molecule concentrations [1]. Also the improved thermal conductivity of such liquids is useful for different particular applications for instance drug delivery, space cooling, transportation, solar energy absorption, nuclear engineering, power generation and several others. There are two models for nanofluids namely the Tiwari and Das model [2] and the Buongiorno's model [3]. According to [3], nanofluid velocity may be observed as the sum of the relative velocity and base fluid (i.e the slip velocity). Also the model provided by [3] is based on the thermophoresis and Brownian diffusion mechanisms. In order to analyze the convective transport in nanofluids several investigators considered this model. For instance, Abbas et al. [4] considered heat generation effects in the hydromagnetic flow of nanofluid induced by a curved stretching sheet. Alsaedi et al. [5] examined the stagnation point flow of nanofluid towards a permeable stretched surface with convective boundary conditions and internal heat generation/absorption. Ziaei-Rad et al. [6] discussed MHD flow of nanofluid by a permeable stretched surface. Heat transfer in MHD stagnation point flow of nanofluid induced by stretching/shrinking surface is analyzed by Nandy and Mahaparta. [7]. Hayat et al. [8] considered magnetohydrodynamics unsteady flow of viscous nanofluid with double stratification. MHD three dimensional flow of nanofluid in presence of convective conditions is studied by Hayat et al. [9]. Mixed convection flow of nanofluid with Newtonian heating is investigated by Hayat et al. [10]. Few more studies on nanofluids and reactive flows can be seen in the refs. [11-22].

The analysis of non-Newtonian materials has engrossed continous consideration of recent investigators. Such consideration is due to their occurrence in geophysics, oil reservoir engineering, bioengineering, chemical and nuclear industries, polymer solution, cosmetic processes, paper production etc. No doubt all non-Newtonian materials on the basis of their behavior in shear are not predicted by one constitutive relationship. This fact of non-Newtonian materials is different than the viscous materials. Thus various models of non-Newtonian fluids have been suggested. Amongst these there is second grade fluid model. No doubt the consideration of second grade fluid predicts the normal stress effects. Moreover heat transfer has awesome part in these fluids. Study of heat transfer characteristics in the stretched flow of non-Newtonian fluids is thus a popular area of research. Turkyilmazoglu [23] studied MHD mixed convection flow of viscoelastic fluid by a permeable stretched surface. Cortell [24] analyzed the flow and heat transfer of second grade fluid with nonlinear radiation and heat generation/absorption. Mukhopadhayay et al. [25] considered the flow of Casson fluid by an unsteady stretching surface. Animasaun et al. [26] examined the nonlinear thermal radiation effects in flow of second grade liquid with homogeneous-heterogeneous reactions. They considered the unequal diffusivities case in this attempt. Hayat et al. [27] presented the MHD three-dimensional flow of nanofluid with velocity slips and nonlinear thermal radiation. Mushtaq et al. [28] explored the nanofluid flow and nonlinear radiative heat transfer with solar energy. Kandasamy et al. [29] studied the impact of solar radiations in flow of viscous material subject to magneto nanoparticles. Ibrahim et al. [30] studied the magnetohydrodynamic (MHD) stagnation point flow of nanofluid with nonlinear radiative heat transfer induced by a stretched surface. Hayat et al. [31] analyzed magnetohydrodynamic (MHD) flow of second grade nanofluid by a nonlinear stretched surface. Reddy et al. [32] considered the Jeffrey liquid flow with torsionally oscillating disks. Das et al. [33] considered MHD Jeffrey liquid and radiative flow by a stretched sheet with surface slip and melting heat transfer. Gao and Jian [34] investigated MHD flow of Jeffrey liquid with circular microchannel. Hayat et al. [35] explored the MHD Jeffrey nanofluid stagnation point flow with Newtonian heating. Narayana and Babu [36] examined the MHD heat and mass transfer of Jeffrey fluid by a stretched surface with thermal radiation and chemical reaction. Nallapu and Radhakrishnamacharya [37] described the Jeffrey liquid flow with narrow tubes in the presence of magnetic field. Farooq et al. [38] presented Jeffrey liquid flow with Newtonian heating and MHD effects. Rao et al. [39] studied the characteristics of heat transfer in flow of second grade liquid induced by non-Isothermal wedge.

The objective of present article is to analyze the stretched flow of viscoelastic fluid with nonlinear radiation and convective boundary conditions. Thus second grade fluid has been dealt with the linearized form of thermal radiation. Homotopy analysis method [40-55] has been implemented for the development of convergent series solution for velocity, temperature and nanoparticle concentration. Graphical results for velocity, temperature and nanoparticle concentration are analyzed for various embedded parameters of interest.

2. Formulation

Here we are interested to analyze the stagnation point flow of viscoelastic nanofluid. Brownian motion and thermophoresis effects are considered. Fluid is electrically conducting in the presence of transversely applied magnetic field B_0. Magnetic Reynolds number is small. Effect of electric field is ignored. Heat transfer through convective condition is discussed. Newly developed boundary condition for mass transfer is imposed. Unlike the classical case, the nonlinear thermal radiation is considered. Physical description of flow is shown in Fig. 1. Applying boundary layer approximation $(o(x)=o(u)=o(1),\ o(y)=o(v)=o(\delta))$ the mathematical problems here are

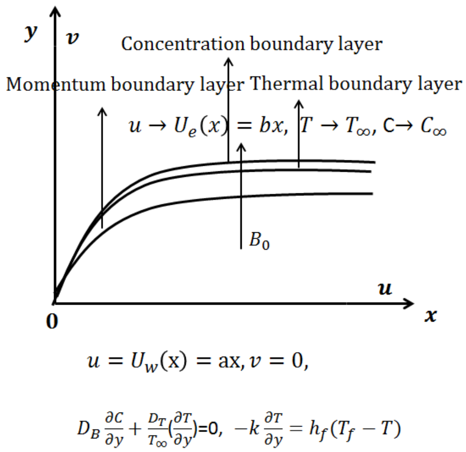

Fig. 1. *Geometry of the Problem.*

$$\frac{\partial u}{\partial x}+\frac{\partial v}{\partial y}=0, \tag{1}$$

$$u\frac{\partial u}{\partial x}+v\frac{\partial u}{\partial y}=U_e\frac{dU_e}{dx}+\frac{\sigma B_0^2}{\rho_f}\left(U_\infty-u\right)+\upsilon\frac{\partial^2 u}{\partial y^2}+k_0\left(\begin{array}{l} u\frac{\partial^3 u}{\partial x\partial y^2}+\frac{\partial u}{\partial x}\frac{\partial^2 u}{\partial y^2} \\ +v\frac{\partial^3 u}{\partial y^3}-\frac{\partial u}{\partial y}\frac{\partial^2 u}{\partial x\partial y}\end{array}\right), \tag{2}$$

$$u\frac{\partial T}{\partial x}+v\frac{\partial T}{\partial y}=\alpha\left(\frac{\partial^2 T}{\partial y^2}\right)+\Gamma\left(D_B\left(\frac{\partial C}{\partial y}\frac{\partial T}{\partial y}\right)+\frac{D_T}{T_\infty}\left[\left(\frac{\partial T}{\partial y}\right)^2\right]\right)-\frac{1}{\rho_f}\frac{\partial q_r}{\partial y}, \tag{3}$$

$$u\frac{\partial C}{\partial x}+v\frac{\partial C}{\partial y}=D_B\left(\frac{\partial^2 C}{\partial y^2}\right)+\frac{D_T}{T_\infty}\left(\frac{\partial^2 T}{\partial y^2}\right), \tag{4}$$

$$u=U_w\left(x\right)=ax,\ v=0,-k\frac{\partial T}{\partial y}=h_f\left(T_f-T\right)\ \text{at}\ y=0,$$

$$D_B\frac{\partial C}{\partial y}+\frac{D_T}{T_\infty}\left(\frac{\partial T}{\partial y}\right)=0\ \text{at}\ y=0,$$

$$u\rightarrow U_e\left(x\right)=bx,\ T\rightarrow T_\infty,\ C\rightarrow C_\infty\ \text{as}\ y\rightarrow\infty. \tag{5}$$

In the aforementioned equations u and v are the velocity components parallel to the x and y directions respectively, U_w the stretching velocity, U_e the free stream velocity, k_0 the viscoelastic parameter, α the thermal diffusivity, Γ the effective heat capacity of nanoparticles, D_B the Brownian diffusion coefficient, D_T the thermophoresis diffusion coefficient, T_∞ the ambient temperature, C_∞ the ambient concentration, ρ_f the density of the fluid, q_r the radiative heat flux and a and b the dimensional constants. Note that the dissipation and Joule heating terms are ignored for low fluid velocity. In view of transformations [30]:

$$\eta = \sqrt{\frac{a}{\upsilon}}y,\ \psi = \sqrt{a\upsilon}xf(\eta),\ u = axf'(\eta),\ v = -\sqrt{a\upsilon}f(\eta),$$

$$\theta(\eta) = \frac{T - T_\infty}{T_f - T_\infty},\ \ \phi(\eta) = \frac{C - C_\infty}{C_\infty}, \tag{6}$$

incompressibility condition given in (1) is automatically satisfied.
Utilizing Rosseland approximation of thermal radiation we get the following expression

$$q_r = -\frac{4\sigma^*}{3k^*}\frac{\partial T^4}{\partial y} = -\frac{16\sigma^*}{3k^*}T^3\frac{\partial T}{\partial y}. \tag{7}$$

In above equation σ^* stands Stefan Boltzmann constant and k^* for mean absorption coefficient. The overhead Eq. (7) is nonlinear in T. Now Eq. (3) yields

$$u\frac{\partial T}{\partial x} + v\frac{\partial T}{\partial y} = \frac{\partial}{\partial y}\left[\left(\alpha + \frac{16\sigma^* T^3}{3(\rho c)k^*}\right)\frac{\partial T}{\partial y}\right] + \Gamma\left(D_B\left(\frac{\partial C}{\partial y}\frac{\partial T}{\partial y}\right) + \frac{D_T}{T_\infty}\left[\left(\frac{\partial T}{\partial y}\right)^2\right]\right). \tag{8}$$

We characterize the non-dimensional temperature $\theta(\eta) = \frac{T - T_\infty}{T_f - T_\infty}$ with $T = T_\infty\left(1 + (Nr - 1)\theta\right)$ and $N_r\left(= \frac{T_f}{T_\infty}\right)$ the temperature ratio parameter. The first term on the right hand side of the above mentioned equation can be simplified as

$$\alpha\left(\frac{\partial}{\partial y}\right)\left(\frac{\partial T}{\partial y}\left(1 + Rd\left(1 + (Nr - 1)\theta\right)^3\right)\right). \tag{9}$$

Here $\mathrm{Rd}\left(= \frac{16\sigma^* T_\infty^3}{3kk^*}\right)$ indicate the radiation parameter and $Rd = 0$ designates no thermal radiation effect.
From Eqs.(2)-(4), (6), (8) and (9) we have

$$f''' + ff'' - f'^2 + A^2 + M^2(A - f') + \gamma\left(2ff''' - ff^{(4)} - f''^2\right) = 0, \tag{10}$$

$$\left[\left(1 + Rd\left(1 + (Nr - 1)\theta\right)^3\right)\theta'\right]' + \Pr\left(f\theta' + Nb\phi'\theta' + Nt\theta'^2\right) = 0, \tag{11}$$

$$\phi'' + Le\Pr f\theta' + \frac{Nt}{Nb}\theta'' = 0, \tag{12}$$

$$\begin{gathered} f(0) = 0,\quad f'(0) = 1,\quad \theta'(0) = Bi\left(\theta(0) - 1\right) \quad \text{at} \quad \eta = 0, \\ Nb\phi'(0) + Nt\theta'(0) = 0, \quad \text{at} \ \ \eta = 0, \\ f'(\infty) = A,\quad \theta(\infty) \to 0,\quad \phi(\infty) \to 0, \ \ \text{as} \quad \eta \to \infty. \end{gathered} \tag{13}$$

Here prime indicates differentiation with respect to η. Moreover $\mathrm{Bi}\left(= \frac{h_f}{k}\sqrt{\frac{\upsilon}{a}}\right)$ represents Biot number, $\Pr\left(= \frac{\upsilon}{\alpha}\right)$ the Prandle number, $\mathrm{A}\left(= \frac{b}{a}\right)$ the ratio parameter, $\gamma\left(= \frac{\upsilon}{ak_0}\right)$ the viscoelastic parameter, $\mathrm{Le}\left(= \frac{\alpha}{D_B}\right)$ the Lewis number, $\mathrm{M}^2\left(= \frac{\sigma B_0^2}{\rho_f a}\right)$ the magnetic parameter, $Nb\left(= \frac{(\rho c)_p D_B C_\infty}{(\rho c)_f \upsilon}\right)$ the Brownian motion parameter, $\mathrm{Rd}\left(= \frac{16\sigma^* T_\infty^3}{3kk^*}\right)$ the radiation parameter, $\mathrm{Nt}\left(= \frac{(\rho c)_p D_T (T_f - T_\infty)}{(\rho c)_f \upsilon T_\infty}\right)$ the thermophoresis parameter and $\mathrm{Nr}\left(= \frac{T_f}{T_\infty}\right)$ the temperature ratio parameter.

Skin friction coefficient and local Nusselt number are

$$C_f = \frac{\tau_w}{\frac{1}{2}\rho U_w^2}, \qquad Nu_x = \frac{x q_w}{k\left(T_f - T_\infty\right)}, \tag{14}$$

where wall shear stress τ_w and wall heat flux q_w are represented in the following expressions

$$\tau_w = \mu\left(\frac{\partial u}{\partial y}\right)_{y=0} + k_0\left(u\frac{\partial^2 u}{\partial x \partial y} + v\frac{\partial^2 u}{\partial y^2} + 2\frac{\partial u}{\partial x}\frac{\partial u}{\partial y}\right), \qquad q_w = -\left(k + \frac{16\sigma^* T^3}{3k^*}\right). \tag{15}$$

Utilizing Eq. (17) in Eq. (16) we obtain

$$\frac{1}{2}C_f\sqrt{\mathrm{Re}_x} = \left(1 + 3\gamma f''(0)\right), \qquad \frac{Nu_x}{\sqrt{\mathrm{Re}_x}} = -\left(1 + Rd\,\theta_w^3 Nr\right)\theta'(0), \tag{16}$$

where $\mathrm{Re}_x = \frac{ax^2}{\upsilon}$ denotes the Reynolds number and Nu_x indicates the local Nusselt number.

3. Series solutions and convergence

Homotopy analysis technique provides us great freedom and an easy way to adjust and control the convergence region of the series solutions. Convergence domain is in the region parallel to $\hbar-$ axis. Therefore we have plotted $\hbar$ -curves in the Figs. 2-3. The admissible ranges of the auxiliary parameters $\hbar_f$, $\hbar_\theta$ and $\hbar_\phi$ are noted [-1.4, -0.1], [-2.2, -0.65] and [-2.0, -0.1].The initial guesses and linear operators relating to the momentum, energy and concentration equations are taken

$$f_0(\eta) = A\eta + 1 + Ae^{-\eta} - A - e^{-\eta},$$

$$\theta_0(\eta) = \frac{Bi}{1+Bi}e^{-\eta}, \qquad \phi_0(\eta) = -\frac{Bi}{1+Bi}\frac{Nt}{Nb}e^{-\eta}, \tag{17}$$

$$£_f = f''' - f', \quad £_\theta = \theta'' - \theta', \quad £_\phi = \phi'' - \phi', \tag{18}$$

$$£_f[C_1^* + C_2^* e^{\eta} + C_3^* e^{-\eta}] = 0, \; £_\theta[C_4^* e^{\eta} + C_5^* e^{-\eta}] = 0, \; £_\phi[C_6^* e^{\eta} + C_7^* e^{-\eta}] = 0, \tag{19}$$

where C_i^* indicate the arbitrary constants.

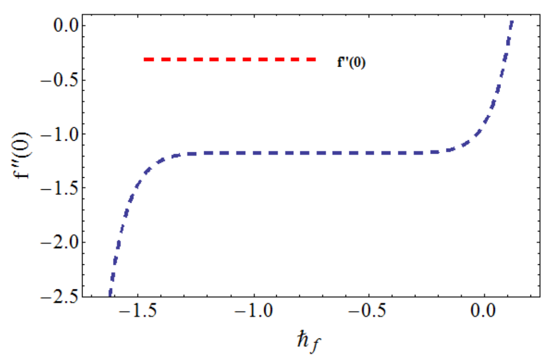

$Fig. 2. h - curve\ for\ f'.$

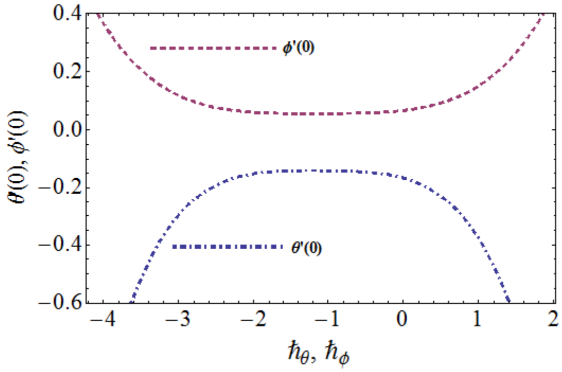

$Fig. 3. h - curves\ for\ \theta\ and\ \phi.$

Table 1: Homotopy solutions convergence when $\gamma = M = Le = 0.1$, Nt = A = λ_2=0.2, Nb = Bi = Rd = 0.5, Nr = 0.7 and Pr = 1.4.

order of approximations	$-f''(0)$	$-\theta'(0)$	$-\phi'(0)$
1	1.1684	0.99704	0.99704
4	1.1711	1.0235	1.0226
9	1.1711	1.0422	1.0439
15	1.1711	1.0575	1.0577
20	1.1711	1.0726	1.0727
25	1.1711	1.0721	1.0720
30	1.1711	1.0721	1.0720

4. Discussion

The main objective of this section is to analyze the behaviors of various involved parameters on the velocity, temperature, concentration, skin friction coefficient and local Nusselt number.

4.1. Velocity distribution

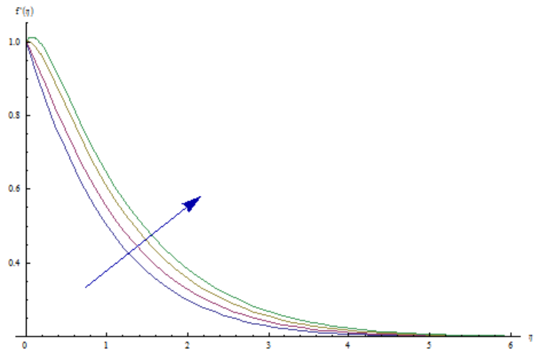

Fig. 4. Impact of γ on f'

when Nb = Bi = Rd = 0.5, $M = Le = 0.1$, Nt = A = λ_2=0.2, Nr = 0.7 and Pr = 1.4.

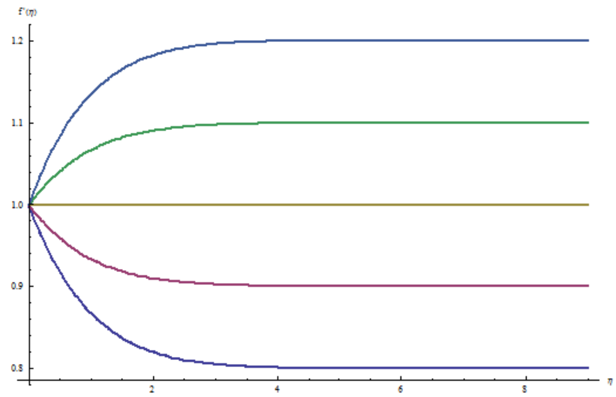

Fig. 5. Impact of A on f'

when Nb = Bi = Rd = 0.5, $\gamma = M = Le = 0.1$, Nt = λ_2=0.2, Nr = 0.7 and Pr = 1.4.

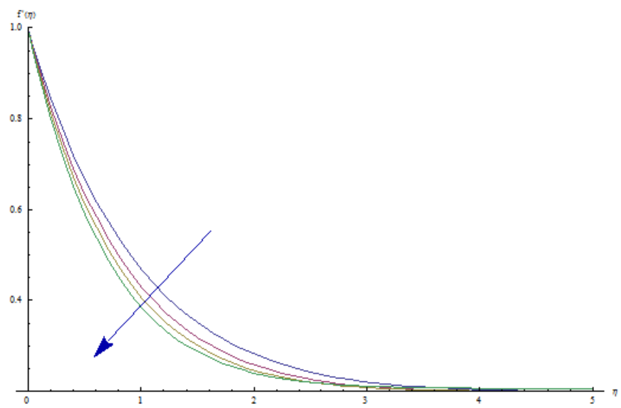

Fig. 6. Impact of M on f'

when Nb = Bi = Rd = 0.5, $\gamma = M = Le = 0.1$, Nt = A = λ_2=0.2, Nr = 0.7 and Pr = 1.4.

Fig. 4 is drawn for different values of viscoelastic parameter γ on the velocity profile. For higher values of γ both velocity distribution and boundary layer thickness increase. Beacuse elasticity of the material increases due to which disturbance occur in material. Thus f' enhances. Fig. 5 is sketched to see the effects of A on velocity distribution. Higher values of A results in enhancement of velocity distribution. It is noted that velocity boundary layer thickness has opposite behavior for A>1 and A<1. For A=1 there exists no boundary layer due to the fact that fluid and sheet move with the same velocity. The behavior of magnetic parameter M on velocity distribution is disclosed through Fig. 6. Here we see that the applied magnetic field slows down the motion of fluid which decreases the velocity.

4.2. Temperature distribution

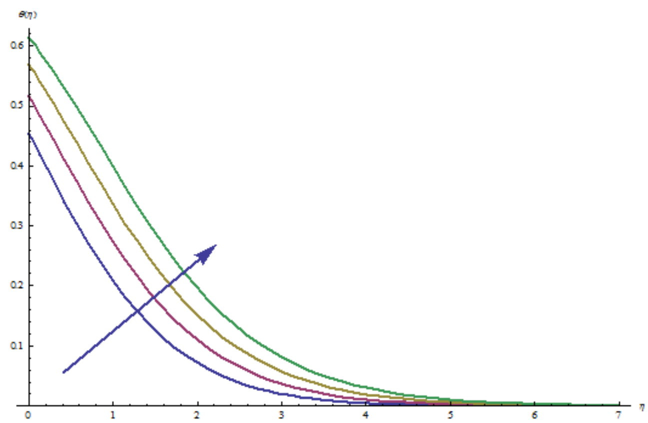

Fig. 7. Impact of Rd on θ

when Nb = Bi = 0.5, $\gamma = M = Le = 0.1$, Nt = A = λ_2=0.2, Nr = 0.7 and Pr = 1.4.

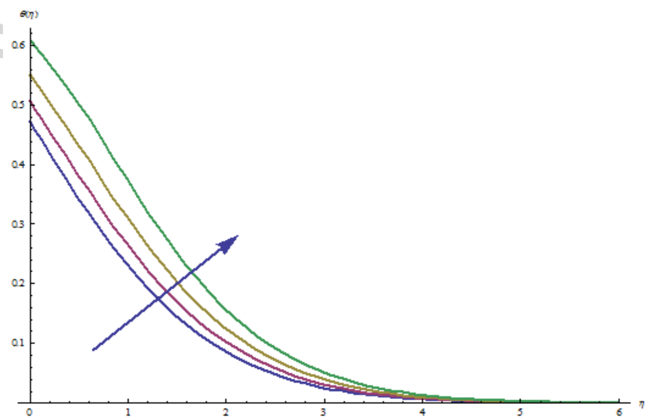

Fig. 8. Impact of Nr on θ

when Nb = Bi = Rd = 0.5, $\gamma = M = Le = 0.1$, Nt = A = λ_2=0.2 and Pr = 1.4.

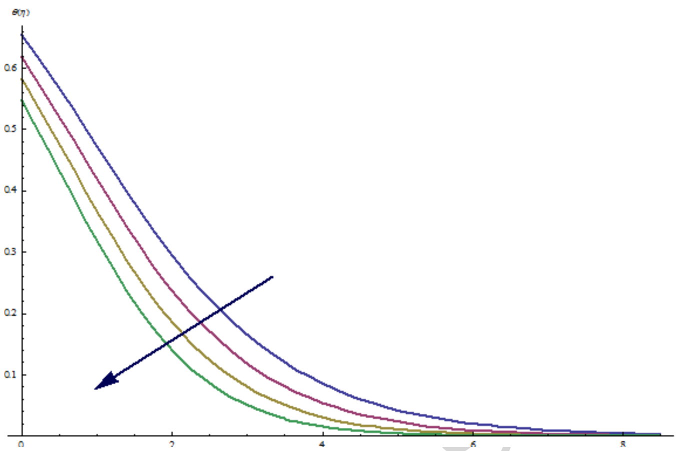

Fig. 9. Impact of Pr on θ

when Nb = Bi = Rd = 0.5, $\gamma = M = Le = 0.1$, Nt = A = λ_2=0.2 and Nr = 0.7 .

Fig. 7 delineates the variation of the temperature in response to a change in the values of radiation parameter Rd. Clearly temperature distribution and the associated thermal boundary layer thickness enhances for large values of radiation parameter Rd. This is due to fact that the surface heat flux increases under the impact of thermal radiation which results in larger temperature inside the boundary layer region. The effects of the temperature ratio parameter Nr on the thermal boundary layer are depicted in Fig. 8. From this Fig.8, it is clear that enhancement in the temperature ratio parameter corresponds to higher wall temperature when compared with ambient fluid. Consequently temperature of the fluid enhances. Moreover, we perceive that the thermal boundary layer thickness increases for the large values of the temperature ratio parameter. Fig. 9 discloses the features of Prandtl number Pr on temperature distribution. It is demonstrated through this Fig. that the temperature and the associated thermal boundary layer thickness are decreasing functions of the Prandtl number. This happens because of the way that the fluids with higher Prandtl number have low thermal conductivity which reduces the conduction and hence the thermal boundary layer thickness.

4.3. Concentration distribution

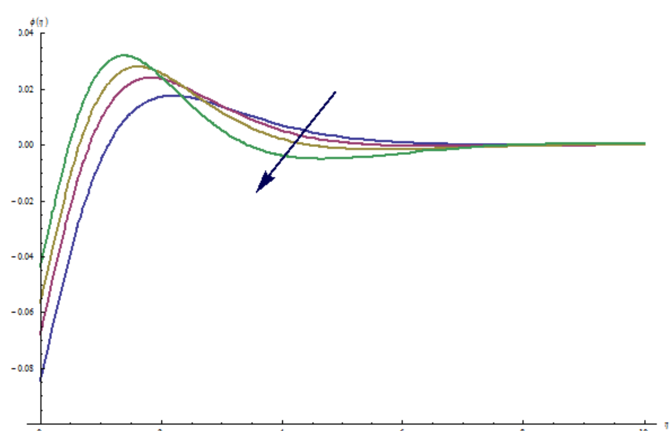

Fig. 10. Impact of Le on ϕ

when Nb = Bi = Rd = 0.5, $\gamma = M = 0.1$, Nt = A = λ_2=0.2, Nr = 0.7 and Pr = 1.4.

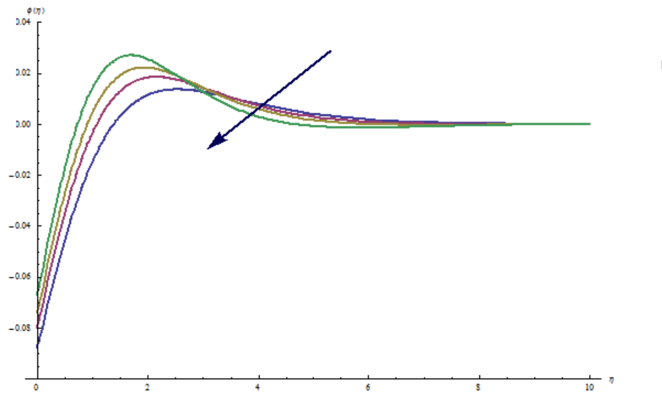

Fig. 11. Impact of Pr on ϕ

when Nb = Bi = Rd = 0.5, $\gamma = M = Le = 0.1$, Nt = A = λ_2=0.2 and Nr = 0.7.

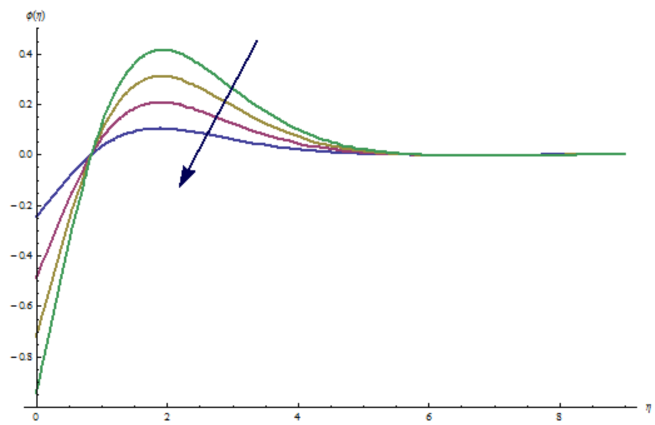

Fig. 12. Impact of Nt on ϕ

when Nb = Bi = Rd = 0.5, $\gamma = M = Le = 0.1$, A = λ_2=0.2, Nr = 0.7 and Pr = 1.4.

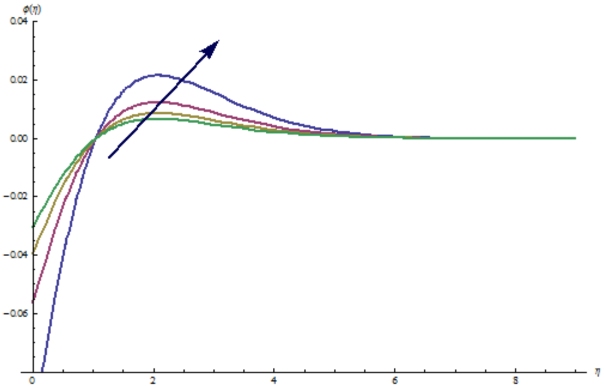

Fig. 13. Impact of Nb on ϕ

when Bi = Rd = 0.5, $\gamma = M = Le = 0.1$, Nt = A = λ_2=0.2, Nr = 0.7 and Pr = 1.4.

Figures 10 and 11 portray characteristics of the Lewis and Prandtl number on the concentration profile. It is evident from figures that intensifying the Prandtl number and Lewis number diminishes concentration profile and associated concentration boundary layer. Moreover, the concentration field is reduced when we increase the values of the Lewis number as it is inversely proportional to the Brownian diffusion coefficient. As Brownian diffusion coefficient is weaker for higher Lewis number and this Brownian diffusion coefficient creates a reduction in the concentration field. Figures 12 and 13 are prepared to put into action, the Brownian motion and thermophoresis parameters on the concentration profile. It is straightforwardly appeared from these figures that the concentration profile and the associated concentration boundary layer thickness builds up for higher thermophoresis parameter while the opposite behavior is observed for the Brownian motion parameter. Physically, the thermophoresis force increments with the increase in thermophoresis parameter which tends to move nanoparticles from hot to cold areas and hence increases the magnitude of nanoparticles volume friction profile. Ultimately the concentration boundary layer thickness turns out to be significantly large for slightly increased value of the thermophoresis parameter. Additionally, higher values of the Brownian motion parameter stifle the diffusion of nanoparticles into the fluid regime away from the surface which as a result decreases the nanoparticles concentration in the boundary layer.

4.4. Skin friction and local Nusselt number

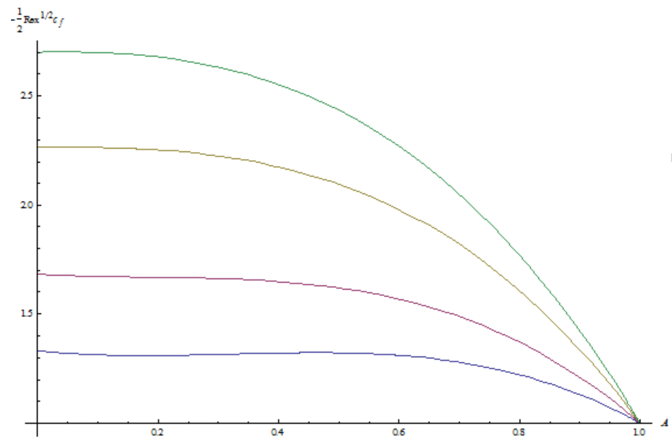

Fig. 14. Impacts of M and A on $\frac{Re_x^{\frac{1}{2}}}{2}C_f$

when Nb = Bi = Rd = 0.5, $\gamma = Le = 0.1$, Nt = λ_2=0.2, Nr = 0.7 and Pr = 1.4.

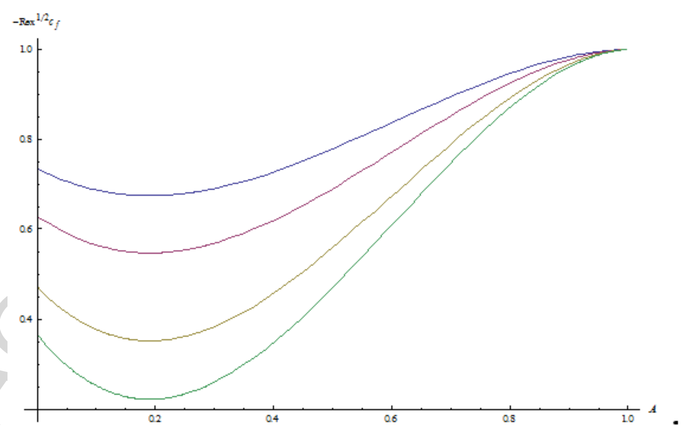

Fig. 15. Impacts of γ and A on $\frac{Re_x^{\frac{1}{2}}}{2}C_f$

when Nb = Bi = Rd = 0.5, $M = Le = 0.1$, Nt = λ_2=0.2, Nr = 0.7 and Pr = 1.4.

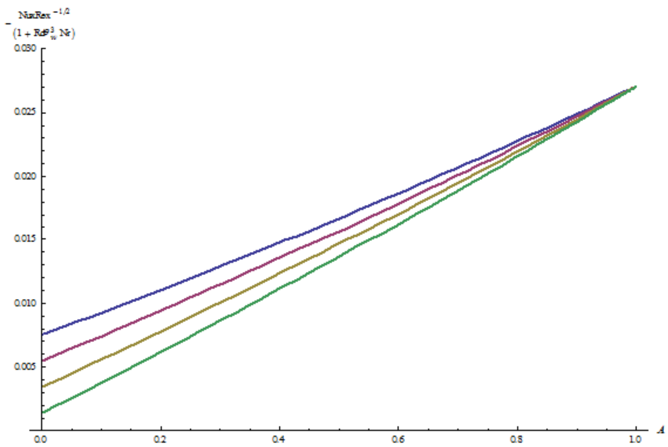

Fig. 16. Impacts of M and A on $-Nu_x Re_x^{-\frac{1}{2}}$

when Nb = Bi = Rd = 0.5, $\gamma = Le = 0.1$, Nt = λ_2=0.2, Nr = 0.7 and Pr = 1.4.

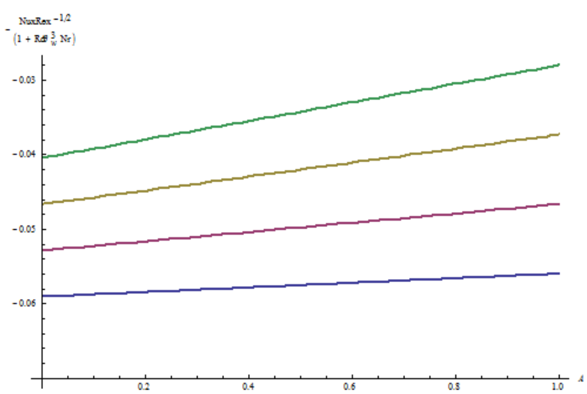

Fig. 17. Impacts of Pr and A on $-Nu_x Re_x^{-\frac{1}{2}}$

when Nb = Bi = Rd = 0.5, $\gamma = M = Le = 0.1$, Nt = λ_2=0.2 and Nr = 0.7.

Skin friction coefficient is plotted for different values of M, A and α in Figs. (14 and 15). Skin friction enhances for higher values of M, A and γ. Figs. (16 and 17) are sketched for Nusselt number with different values of M, A and Pr. It is analyzed that Nusselt number enhances for larger values of M, A and Pr. Table 1 shows the convergence of series solutions of momentum, energy and concentration equations. It is noted that 25^{th} and 30^{th} order of approximations are sufficient for the convergence of momentum, energy and concentration equations, respectively.

5. Conclusions

Here we explored the impact of passive control of nanoparticles in the stagnation point flow of viscoelastic fluid. The key points are summarized as follows:

- Nanoparticles concentration distribution decreases for an increase in Nb while it enhances for larger values of Nt.

- The thermal and concentration boundary layer thicknesses are enhanced while the rate of heat transfer is decreased by increasing values of thermophoresis parameter.
- With the increasing Brownian motion parameter the concentration profile is decreased however the temperature and rate of heat transfer remained unaffected.
- Skin friction coefficient is increasing function of M, A and γ.
- Radiation parameter Rd favors the thermal boundary layer thickness.

References

1. S. U. S. Choi, Enhancing thermal conductivity of fluids with nanoparticles, ASME Fluids Eng. Div. 231 (1995) 99-105.
2. R. K. Tiwari and M. K. Das, Heat transfer augmentation in a two-sided lid driven differentially heated square cavity utilizing nanofluids, Int. J. Heat Mass Transfer 50 (2007) 2002 – 2018.
3. J. Buongiorno, Convective transport in nanofluids, ASME J. Heat Transfer 128 (2006) 240 – 250.
4. Z. Abbas, M. Naveed and M. Sajid, Heat generation effects in the hydromagnetic flow of nanofluid induced by a curved stretching, J. Mol. Liquids 215 (2016) 756--762.
5. A. Alsaedi, M. Awais and T. Hayat, Effects of heat generation/absorption on stagnation point flow of nanofluid over a surface with convective boundary conditions, Commu. Nonlinear Sci. Numer. Simulat. 17 (2012) 4210--4223.
6. M. Ziaei-Rad, M. Saeedan and E. Afshari, Simulation and prediction of MHD dissipative nanofluid flow on a permeable stretching surface using artificial neural network, Appl. Thermal Eng 99 (2016) 373--382.
7. S. K. Nandy and T. R. Mahapatra, Effects of slip and heat generation/absorption on MHD stagnation flow of nanofluid past a stretching/shrinking surface with convective boundary conditions, Int. J. Heat Mass Transf. 64 (2013) 1091--1100.
8. T. Hayat, M. Imtiaz and A. Alsaedi, Unsteady flow of nanofluid with double stratification and magnetohydrodynamics, Int. J. Heat Mass Transf. 92 (2016) 100--109.
9. T. Hayat, M. Imtiaz and A. Alsaedi, MHD 3D flow of nanofluid in presence of convective conditions, J. Mol. Liq. 212 (2015) 203--208.
10. M, Imtiaz, T. Hayat, M. Hussain, S. A. Shehzad, G. Q. Chen and B. Ahmad, Mixed convection flow of nanofluid with Newtonian heating, Eur. Phys. J. Plus 129 (2014) 97.
11. T. Hayat, M. I. Khan, M. Farooq, A. Alsaedi, M. Waqas and T. Yasmeen, Impact of Cattaneo--Christov heat flux model in flow of variable thermal conductivity fluid over a variable thicked surface, Int. J. Heat Mass Transf. 99 (2016) 702-710.
12. T. Hayat, M. I. Khan, M. Farooq, T. Yasmeen and A. Alsaedi, Stagnation point flow with Cattaneo-Christov heat flux and homogeneous-heterogeneous reactions, J. Mol. Liquids. 220 (2016) 49-55.
13. T. Hayat, M. Waqas, S. A. Shehzad and A. Alsaedi, A model of solar radiation and Joule heating in magnetohydrodynamic (MHD) convective flow of thixotropic nanofluid, J. Mol. Liquids 215 (2016) 704-710.
14. T. Hayat, M. Waqas, S. A. Shehzad and A. Alsaedi, Mixed convection flow of viscoelastic nanofluid by a cylinder with variable thermal conductivity and heat source/sink, Int. J. Numer. Methods Heat Fluid Flow 26 (2016) 214-234.

15. M. J. Babu, N. Sandeep and C. S. K Raju, Heat and Mass transfer in MHD Eyring-Powell nanofluid flow due to cone in porous medium, Int. J. Eng. Resear. Africa, 19(2016) 57-74.
16. W.A. Khan, O.D. Makinde and Z.H. Khan, Non-aligned MHD stagnation point flow of variable viscosity nanofluids past a stretching sheet with radiative heat, Int. J. Heat Mass Transf. 96 (2016) 525--534.
17. O.D. Makinde, F. Mabood, W.A. Khan and M.S. Tshehla, MHD flow of a variable viscosity nanofluid over a radially stretching convective surface with radiative heat, J. Mol. Liq. 219 (2016) 624--630.
18. O.D. Makinde, W.A. Khan and J.R. Culham, MHD variable viscosity reacting flow over a convectively heated plate in a porous medium with thermophoresis and radiative heat transfer, Int. J. Heat Mass Transf. 93 (2016) 595--604.
19. W. A. Khan, J. R. Culham and O. D. Makinde, Combined heat and mass transfer of third-grade nanofluids over a convectively-heated stretching permeable surface, Can. J. Chem. Eng. 93 (2015) 1880--1888.
20. W. A. Khan, J. R. Culham and O. D. Makinde ,Hydromagnetic blasius flow of power-law nanofluids over a convectively heated vertical plate, Can. J. Chem. Eng. 93 (2015) 1830--1837.
21. O.D. Makinde, W.A. Khan and Z.H. Khan, Buoyancy effects on MHD stagnation point flow and heat transfer of a nanofluid past a convectively heated stretching/shrinking sheet, Int. J. Heat Mass Transf. 62 (2013) 526--533.
22. T. Hayat, Z. Hussain, A. Alsaedi and B. Ahmad, Heterogeneous-homogeneous reactions and melting heat transfer effects in flow with carbon nanotubes, J. Mol. Liq. 220 (2016) 200–207.
23. M. Turkyilmazoglu, The analytical solution of mixed convection heat transfer and fluid flow of a MHD viscoelastic fluid over a permeable stretching surface, Int. J. Mech. Sci. 77 (2013) 263-268.
24. R. Cortell, MHD (magneto-hydrodynamic) flow and radiative nonlinear heat transfer of a viscoelastic fluid over a stretching sheet with heat generation/absorption, Energy 74 (2014) 896-905.
25. S. Mukhopadhyay, P. R. De, K. Bhattacharyya, G.C. Layek, Casson fluid flow over an unsteady stretching surface, Ain Sham. Eng. J. 4 (2013) 933-938.
26. L. Animasaun, C. S. K. Raju and N. Sandeep, Unequal diffusivities case of homogeneous--heterogeneous reactions within viscoelastic fluid flow in the presence of induced magnetic-field and nonlinear thermal radiation, Alex. Eng. J. (2016) (In Press)
27. T. Hayat, M. Imtiaz, A. Alsaedi and M. A. Kutbi, MHD three-dimensional flow of nanofluid with velocity slip and nonlinear thermal radiation, J. Magn. Magn. Mater. 396 (2015) 31--37.
28. A. Mushtaq, M. Mustafa, T. Hayat and A. Alsaedi, Nonlinear radiative heat transfer in the flow of nanofluid due to solar energy: A numerical study, J Taiwan Inst Chem Eng. 45 (2014) 1176-1183.
29. R. Kandasamy, I. Muhaimin and R. Mohamad, Thermophoresis and Brownian motion effects on MHD boundary-layer flow of a nanofluid in the presence of thermal stratification due to solar radiation, Int. J. Mech. Sci. 70 (2013) 146-154.
30. W. Ibrahim, Nonlinear radiative heat transfer in magnetohydrodynamic (MHD) stagnation point flow of nanofluid past a stretching sheet with convective boundary

condition, Prop Pow. Res. 4 (2015) 230-239.

31. T. Hayat, M. Waqas, S. A. Shehzad and A. Alsaedi, Mixed convection flow of viscoelastic nanofluid by a cylinder with variable thermal conductivity and heat source/sink, Int. J. Numer. Methods Heat Fluid Flow 26 (2016) 214-234.
32. G. B. Reddy, S. Sreenadh, R. H. Reddy and A. Kavitha, Flow of a Jeffrey fluid between torsionally oscillating disks, Ain Sham. Eng. J. 6 (2015) 355-362.
33. Das, N. Acharya and P. K. Kundu, Radiative flow of MHD Jeffrey fluid past a stretching sheet with surface slip and melting heat transfer, Alex. Eng. J. 54 (2015) 815-821.
34. C. Gao and Y. Jian, Analytical solution of magnetohydrodynamic flow of Jeffrey fluid through a circular microchannel, J. Mol. Liq. 211 (2015) 803-811.
35. T. Hayat, M. Imtiaz and A. Alsaedi, Magnetohydrodynamic stagnation point flow of a Jeffrey nanofluid with Newtonian heating, J. Aerospace Eng. (2015) 10.1061/(ASCE)AS.1943-5525.0000568, 04015063.
36. P. V. S. Narayana and D. H. Babu, Numerical study of MHD heat and mass transfer of a Jeffrey fluid over a stretching sheet with chemical reaction and thermal radiation, J. Taiwan Ins. Chem. Eng. 59 (2016) 18-25.
37. S. Nallapu and G. Radhakrishnamacharya, Jeffrey fluid flow through a narrow tubes in the presence of a magnetic field, Procedia Eng. 127 (2015) 185--192.
38. M. Farooq, N. Gull, A. Alsaedi and T. Hayat, MHD flow of a Jeffrey fluid with Newtonian heating, J. Mech. 33 (03) (2015) 1 - 11.
39. A. S. Rao, N. Nagendra and V. R. Prasad, Heat Transfer in a non-Newtonian Jeffrey's fluid over a non-Isothermal wedge, Procedia Eng. 127 (2015) 775-782.
40. S. J. Liao, Homotopy analysis method in nonlinear differential equations, Springer & Higher Education Press, 2012.
41. T. Hayat, M. Imtiaz and A. Alsaedi, Impact of magnetohydrodynamics in bidirectional flow of nanofluid subject to second order slip velocity and homogeneous-heterogeneous reactions, J. Magn. Magn. Mater. 395 (2015) 294-302.
42. T. Hayat, M. Waqas, S. A Shehzad and A. Alsaedi, Mixed convection radiative flow of Maxwell fluid near a stagnation point with convective condition, J. Mech. 29 (2013) 403 – 409.
43. T. Hayat, S. Asad, M. Mustafa and A. Alsaedi, MHD stagnation point flow of Jeffrey fluid over a convectively heated stretching sheet, Comput. Fluids 108 (2015) 179 – 185.
44. Y. Lin and L. Zheng, Marangoni boundary layer flow and heat transfer of copper-water nanofluid over a porous medium disk, AIP Adv. 5 (2015) 107225.
45. Sui, L. Zheng, X. Zhang and G. Chen, Mixed convection heat transfer in power law fluids over a moving conveyor along an inclined plate, Int. J. Heat Mass Transf. 85 (2015) 1023 - 1033.
46. T. Hayat, U. Shaheen, A. Shafiq, A. Alsaedi and S. Asghar, Marangoni mixed convection flow with Joule heating and nonlinear radiation, AIP Adv. 5 (2015) 077140.
47. S. Noeiaghdam, E. Zarei and H. B. Kelishami, Homotopy analysis transform method for solving Abel's integral equations of the first kind, Ain Shams Eng. J. 2015 (in press).
48. F. Mirzaee, M. K. Yari and M. Paripour, Solving linear and nonlinear Abel fuzzy integral equations by homotopy analysis method, J. Taibah Uni. Sci. 9 (2015) 104-115.
49. M.I. Khan, M. Z. Kiyani, M. Y. Malik, T. Yasmeen, M. W. A. Khan and T. Abbas, Numerical investigation of magnetohydrodynamic stagnation point flow with variable properties, Alex. Eng. J. DOI: 10.1016/j.aej.2016.04.037.

50. M. Waqas, M. I. Khan, M. Farooq, A. Alsaedi, T. Hayat and T. Yasmeen, Magnetohydrodynamic (MHD) mixed convection flow of micropolar liquid due to nonlinear stretched sheet with convective condition. Int. J. Heat Mass Transf. (2016) (in press).
51. T. Hayat, M. Rashid, M. Imtiaz and A. Alsaedi, Magnetohydrodynamic (MHD) stretched flow of nanofluid with power-law velocity and chemical reaction, AIP Advances. 5 (2015) 117121.
52. T. Hayat, M. Imtiaz and A. Alsaedi, Effects of homogeneous-heterogeneous reactions in flow of Powell-Eyring fluid, J. Cent. South Univ. 22 (2015) 3211-3216.
53. T. Hayat, M. Waqas, S. A. Shehzad and A. Alsaedi, MHD stagnation point flow of Jeffrey fluid by a radially stretching surface with viscous dissipation and Joule heating, J. Hydrology Hydromech. 63 (2016) 311-317.
54. T. Hayat, S. Farooq, B. Ahmad and A. Alsaedi, Characteristics of convective heat transfer in the MHD peristalsis of Carreau fluid with Joule heating, AIP Advances 6 (2016) 045302.
55. T. Hayat, S. Qayyum, M. Imtiaz and A. Alsaedi, Three-dimensional rotating flow of Jeffrey fluid for Cattaneo-Christov heat flux model, AIP Advances 6 (2016) 025012.

Highlights

Non-linear thermal radiation effect is observed with viscoelastic nanofluid.

Characteristics of heat transfer are explored in the presence convective boundary condition.

Skin friction and Nusselt number have been numerically analyzed.